Supporting Information

Metal coordination strategy to control the pore structure of hard carbon materials for high-performance sodium storage

Wenbo Hou[a], Bo Tao[a], Lili Ma[a], Zhiyuan Liu[a], Yawen Ren[a], Hui peng[a,*], Guofu Ma[a,*]

[a]Key Laboratory of Eco-Functional Polymer Materials of the Ministry of Education, Key Laboratory of Polymer Materials of Gansu Province, College of Chemistry and Chemical Engineering, Northwest Normal University, Lanzhou 730070, China.

*Corresponding authors. E-mail: penghui@nwnu.edu.cn (H. Peng), magf@nwnu.edu.cn (G. Ma).

S1 Experimental

S1.1 Materials synthesis

Zinc acetate ($Zn(AC)_2$), aniline, ammonium persulfate (APS), and carboxymethyl cellulose (CMC) were purchased from Aladdin Biochemical Technology Co., Ltd. (China).

0.3 g of CMC was dissolved in a mixed solution of 90 mL of deionized water and 30 mL of 1 M HCl until it was completely dissolved at room temperature. The mixed CMC solution was transferred to an ice-water bath (below 5 ℃), and then 1.2 g of aniline monomer and 0.1 g of $Zn(AC)_2$ were added to the solution and stirred for 30 min. Subsequently, 3.75 g of APS was added to the above mixture and polymerized in an ice-water bath for 6 h. The precipitate was collected by centrifugation and washed with deionized water and ethanol several times to remove APS and oligoaniline. Finally, it was dried at 60 ℃ for 12 h to obtain polyaniline (Zn-PANI) coordinated with zinc acetate. At the same time, polyaniline (PANI) was prepared by the same method without $Zn(AC)_2$.

PANI and Zn-PANI powders were heated to 450 ℃ at a heating rate of 5 ℃ min^{-1} in a tube furnace under nitrogen atmosphere for 2 h. Then the temperature was raised to 1300 ℃ at a heating rate of 3 ℃ min^{-1} and maintained for 2 h to obtain nitrogen-containing hard carbon materials, which were recorded as HC and Zn-HC, respectively.

S1.2 Materials characterization

The morphology of the products was examined by field emission scanning electron microscopy (FE-SEM, Ultra Plus, Carl Zeiss, Germany) at an accelerating voltage of 5.0 kV. The microstructure of the samples was characterized by transmission electron microscopy (TEM, Carl Zeiss, Germany). The Brunner-Emmet-Taylor (BET) surface area (S_{BET}) of the samples was analyzed by adsorption and desorption in N_2 (77 K) atmospheres on Micromeritics ASAP 2460 nitrogen adsorber in the United States. Prior to nitrogen adsorption measurements, all samples were degassed at 300 °C. X-ray diffraction (XRD) of the samples was performed on an advanced diffractometer (D/Max-2400, Rigaku) using Cu Kα radiation (k = 1.5418 Å), 40 kV, 100 mA. The 2θ range used in the measurements

was to 80°. X-ray photoelectron spectroscopy (XPS) measurements were performed on a K-Alpha system (USA) using a monochromatic Al Kα radiation source. Raman spectroscopy was conducted by employing a Horiba Scientific LabRAM HR-Evolution. Fourier transform infrared spectra were collected on a Fourier transform infrared spectrometer (FTIR, Bruker tensor 27, Germany). Thermogravimetric analysis (TG) is performed on a Netzsch instrument. In N_2 atmosphere, the pyrolysis behavior of the materials was analyzed in the range of 50-800 ℃ at the temperature of 20 ℃ min^{-1}.

S1.3 Electrochemical characterization

For the fabrication of Zn-HC anode, 80 wt% of Zn-HC active material, 10 wt% of Super P and 10 wt% of polyvinylidene fluoride (PVDF) were mixed in N-methyl-2-pyrrolidone (NMP), and then the mixed slurry was uniformly coated on a copper foil, which was dried in a vacuum drying oven at 80 ℃ overnight. Subsequently, the coated copper foil was cut into circular electrode sheets of 12 mm in diameter under the pressure of 10 M Pa. The mass of the active material of the electrode sheet was 0.8-1.0 mg.

The electrode sheets were assembled to half-cell in a CR2032 coin cell in a glove box filled with Ar atmosphere with a content of H_2O and O_2 lower than 0.1 ppm using a sodium foil with a diameter of 15.6 mm as the reference electrode and 1 M $NaPF_6$ in DME (100 Vol%) as electrolyte.

To make the full cell, the Zn-HC anode was first charged and discharged several times at a current density of 0.02 A g^{-1}. The pre-sodiumized HC anode was then stripped in a glove box. Then, the HC anode and NVP@C cathode were assembled in a CR2032 coin cell using glass fiber (Whatman, GF/D) and 1 M $NaPF_6$ in DME (100 Vol%) as separator and electrolyte, respectively.

S1.4 Electrochemical measurements

Cyclic voltammetry (CV) test, galvanostatic charge/discharge measurements and electrical impedance spectroscopy (EIS) test were recorded by a CHI760E (Shanghai, China). Life-span tests for half-cell and hybrid cells used a battery test system (Land CT200lA model, Wuhan Land

Electronics, Ltd.).

GITT was considered to an effective method for evaluating the apparent diffusion coefficient of ions at different equilibrium potentials. The Na^+ diffusion coefficient (D_K) can be calculated according to Fick's second law with the equation:

$$D_{K^+} = 4(m_b V_m / M_b S)^2 (\Delta E_S / \Delta E\tau)^2 / \pi\tau$$

where τ is the relaxation time of the electrode, m_b, M_b, V_m and S denote the mass of electrode active material, molar volume, molar mass, and electrode area of the electrode active substance, respectively. ΔE_S and ΔE_τ represent voltage changes caused by the galvanostatic current discharge and pulse, respectively.

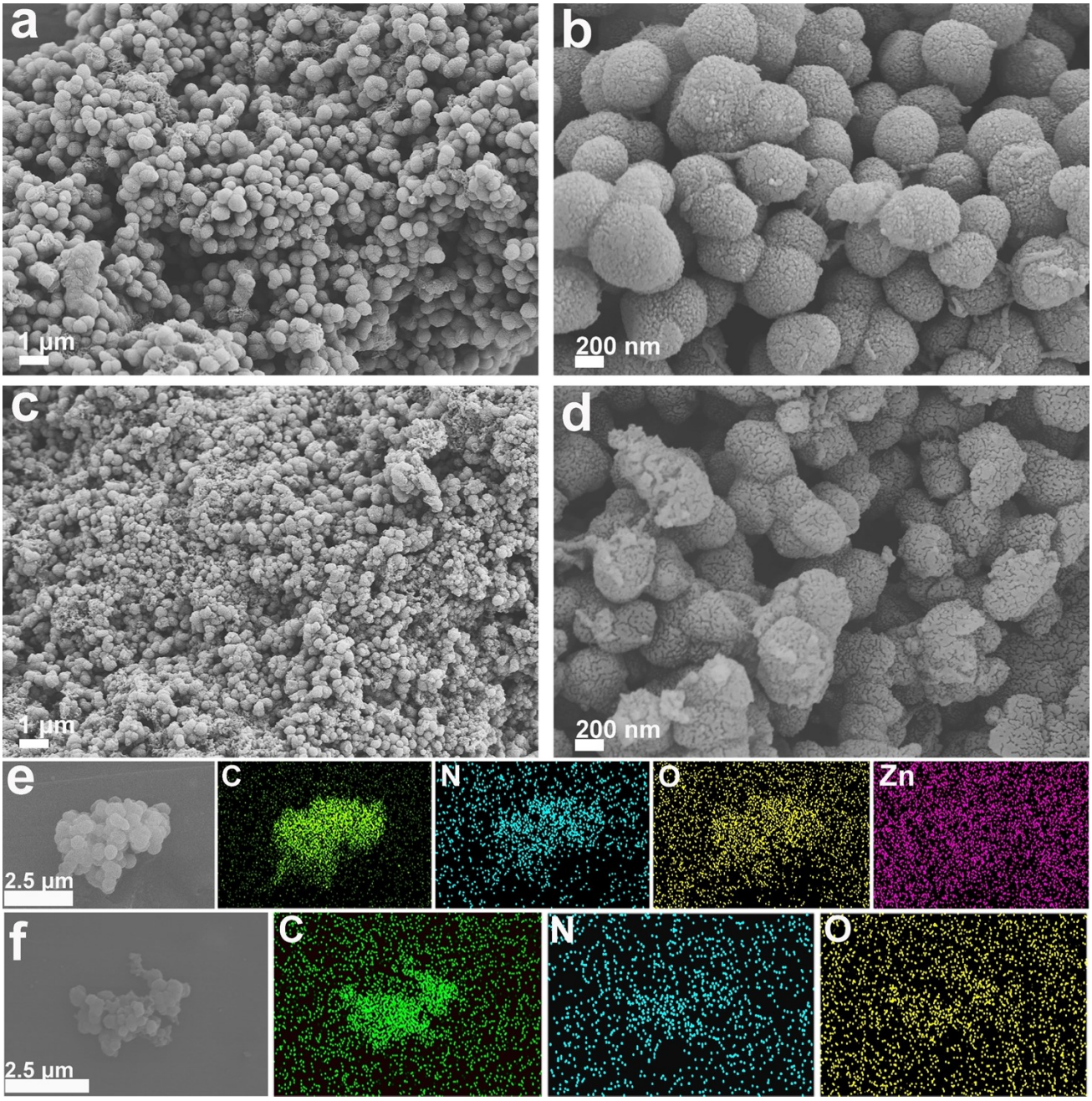

Fig. S1. SEM of (a-b) Zn-PANI, (c-d) PANI, (e-f) Energy-dispersive X-ray spectroscopy mapping images for Zn-PANI and PANI.

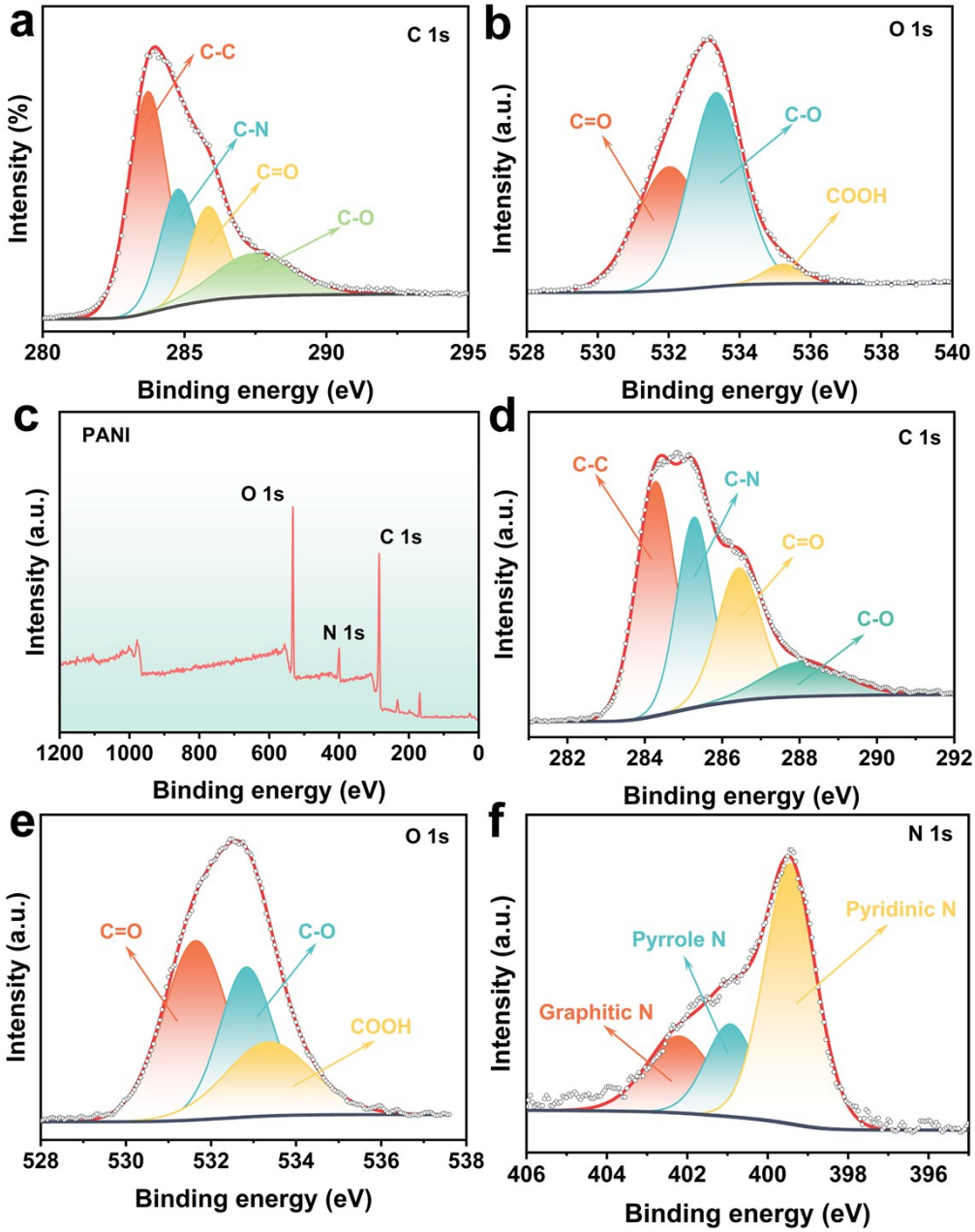

Fig. S2. The high-resolution XPS spectra of (a) C 1s, (b) O 1s for Zn-PANI. (c) The full XPS spectra of PANI. The high-resolution XPS spectra of (d) C 1s, (e) O 1s, (f) N 1s for PANI.

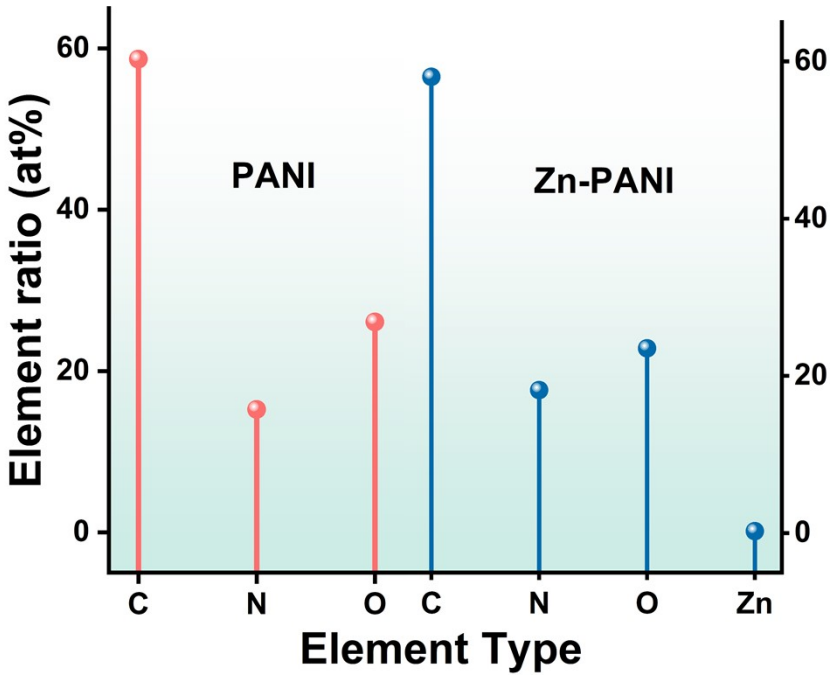

Fig. S3. Atomic ratios of elements C, N, O, and Zn in Zn-PANI and PANI from XPS.

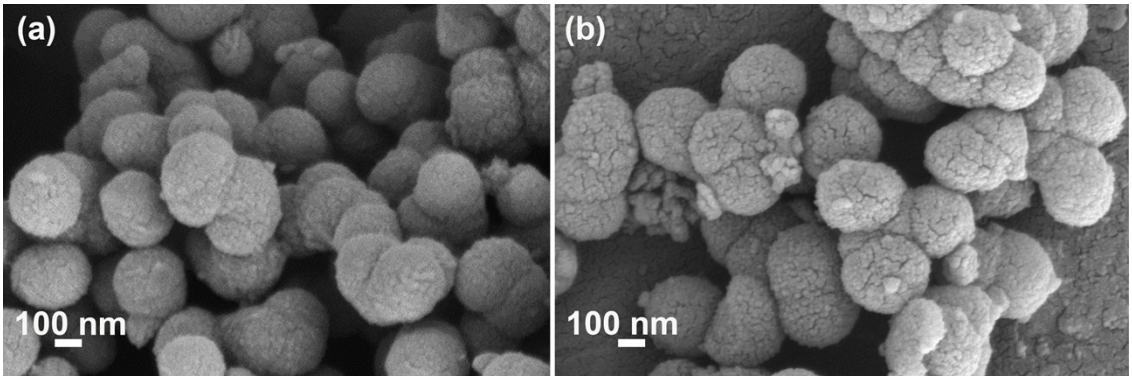

Fig. S4. SEM images of (a) HC, (b) Zn-HC

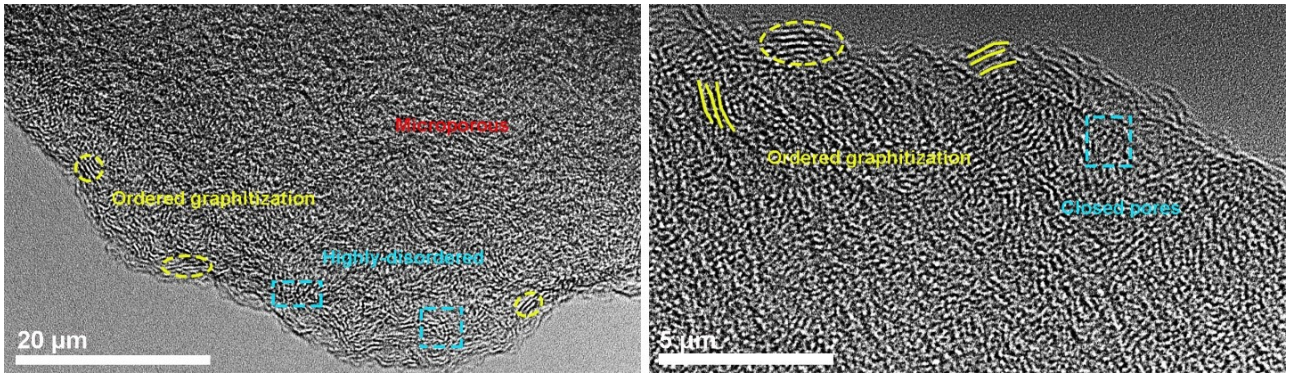

Fig. S5 HRTEM images of HC.

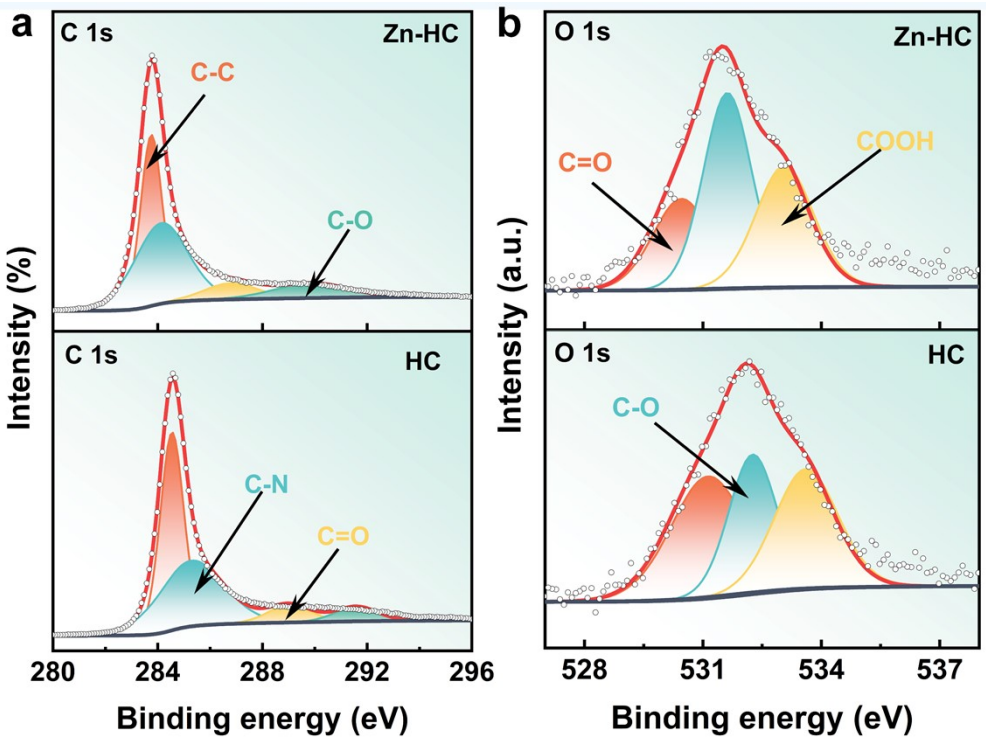

Fig. S6. The high-resolution XPS spectra for Zn-HC and HC. (a) C 1s, (b) O 1s.

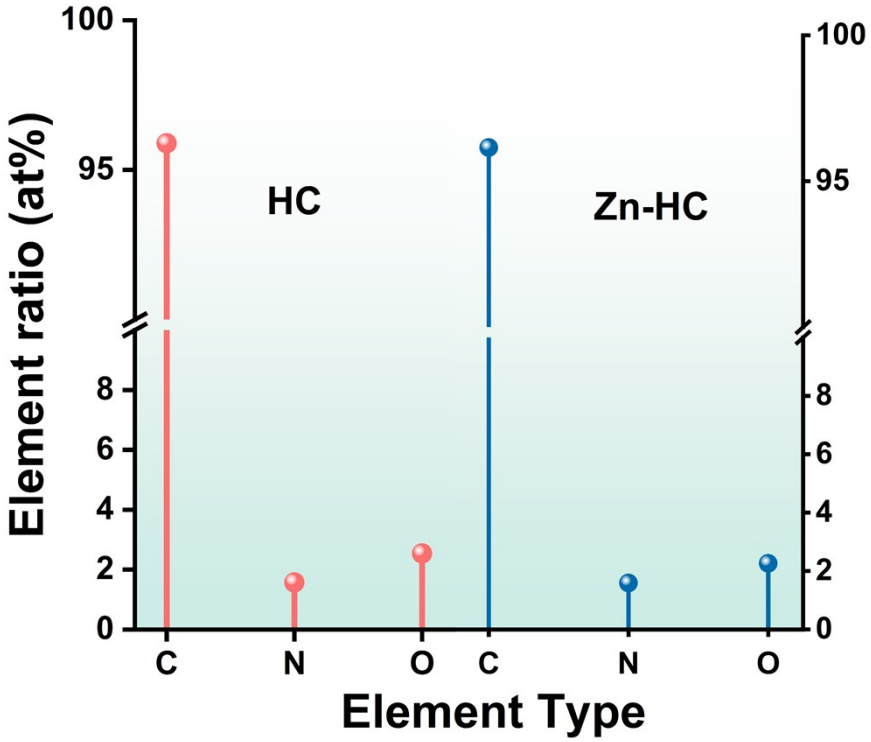

Fig. S7. Atomic ratios of elements C, N and O in Zn-HC and HC from XPS.

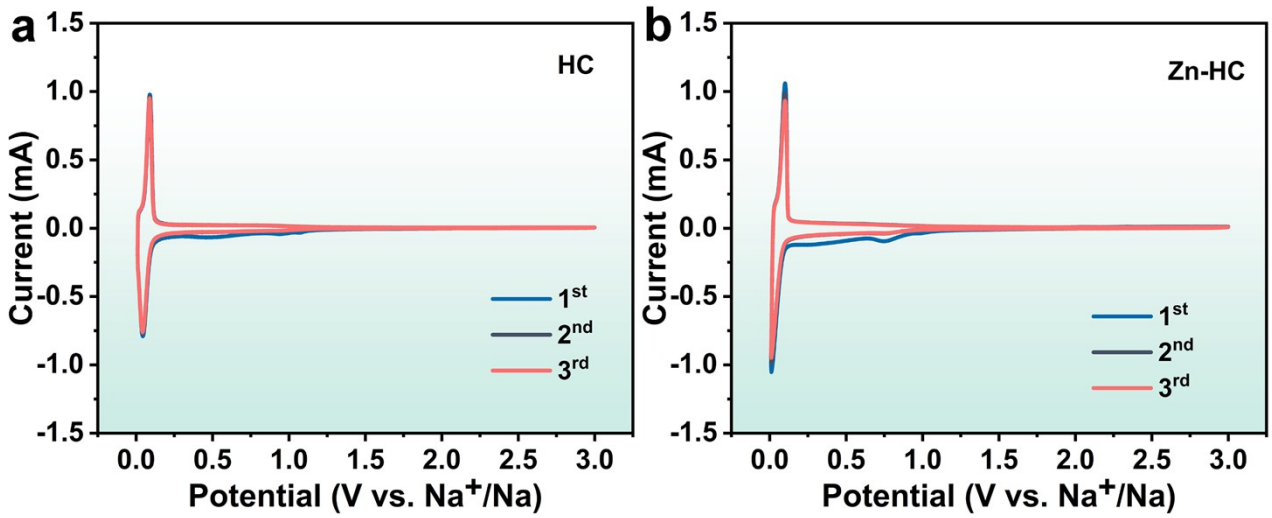

Fig. S8. CV curves of (a) HC and (b) Zn-HC.

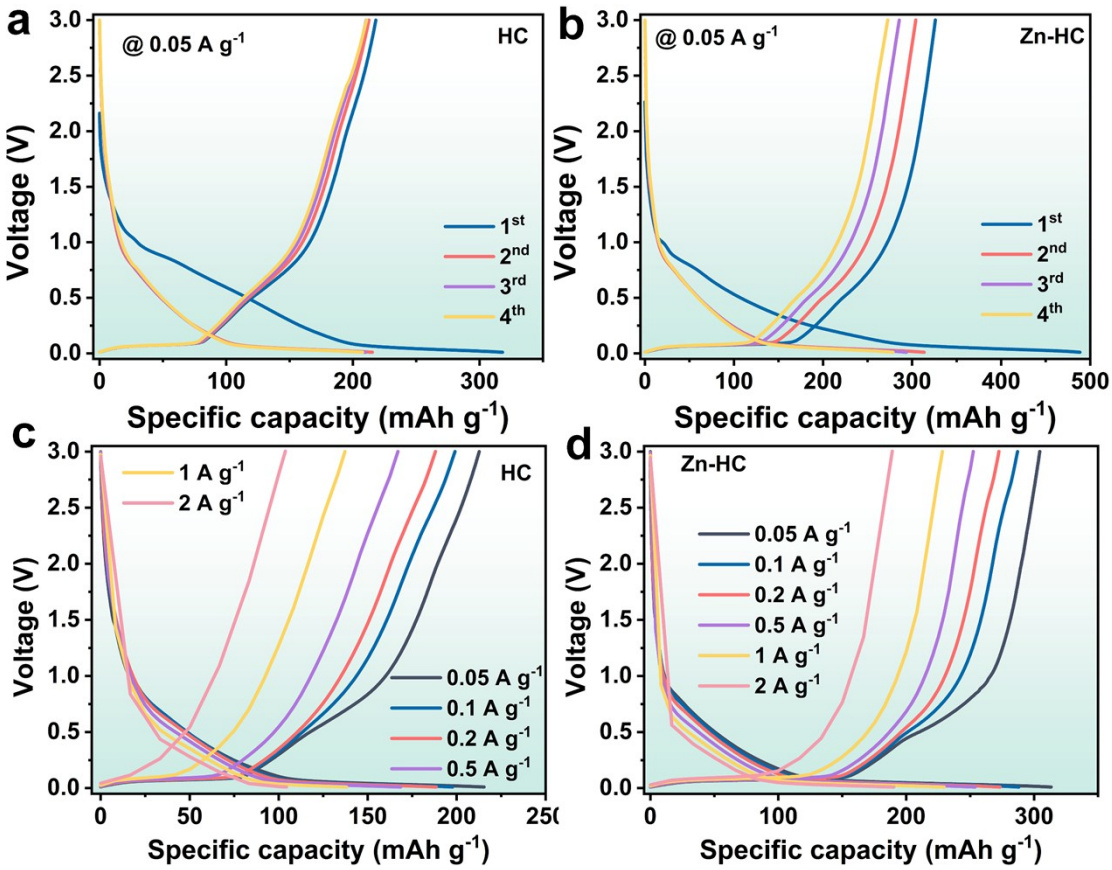

Fig. S9. GCD curves of (a) HC and (b) Zn-HC for first four cycles at 0.05 A g^{-1}, GCD curves of (c) HC and (d) Zn-HC at different current densities.

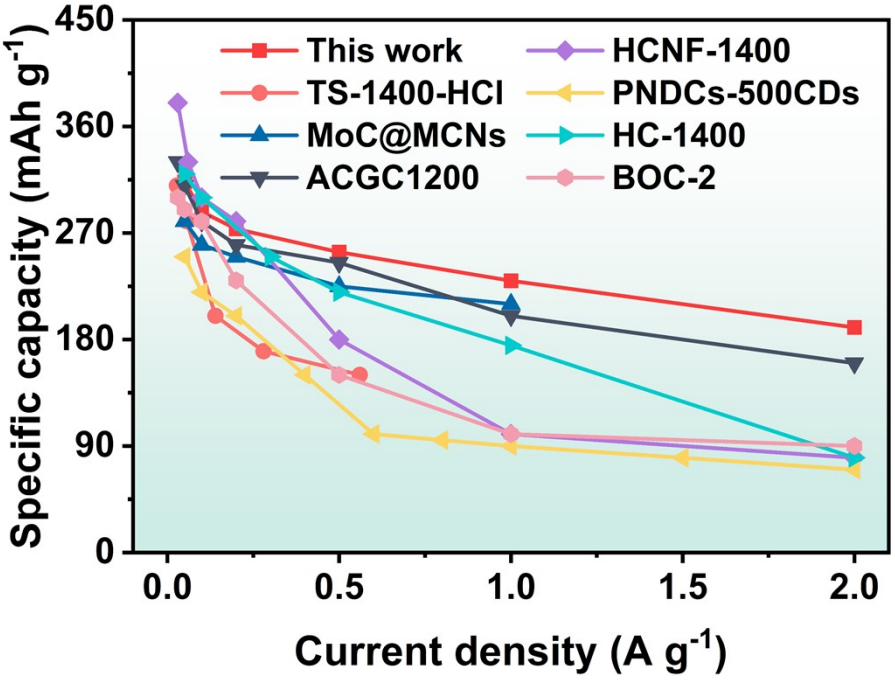

Fig. S10. Electrochemical properties comparison of the Zn-HC and previously reported carbon.[1-7]

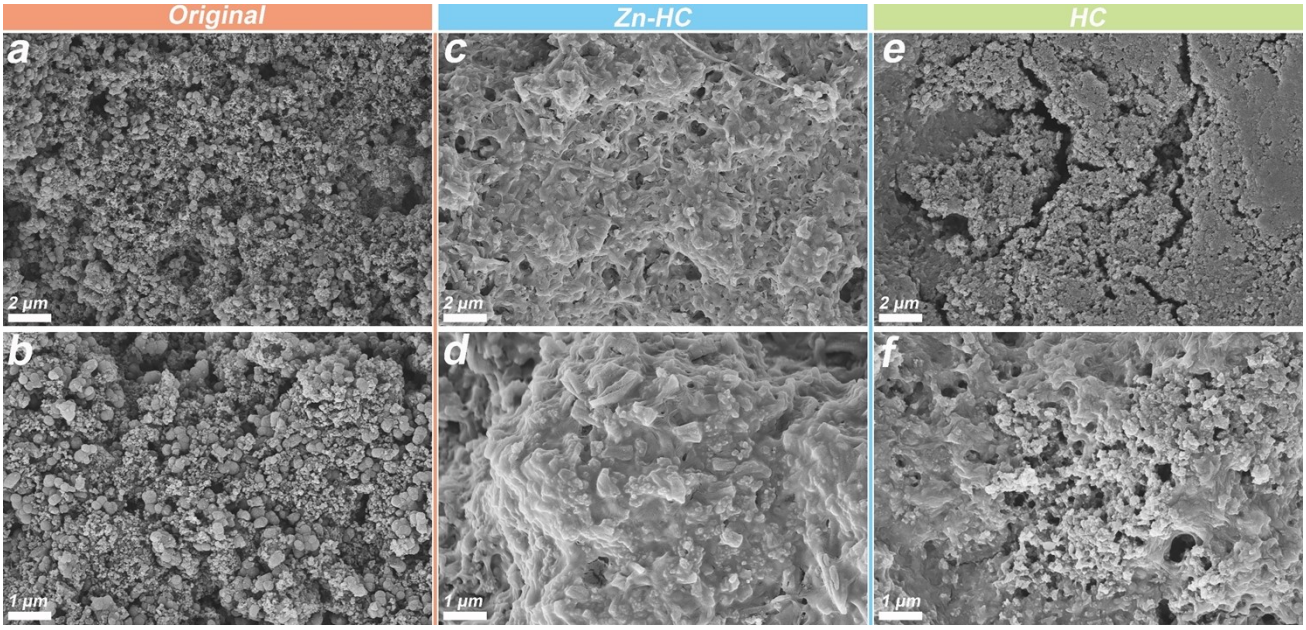

Fig. S11. Ex-situ SEM images, (a-b) original electrode, after 500 cycles (c-d) Zn-HC and (e-f) HC.

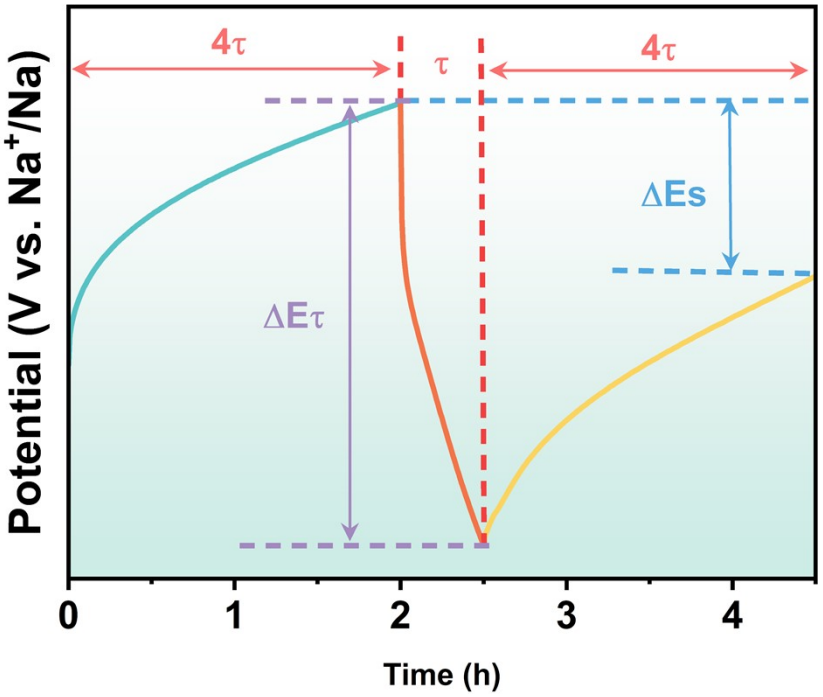

Fig. S12. Schematic diagram of basic parameters of GITT analysis within one cycle.

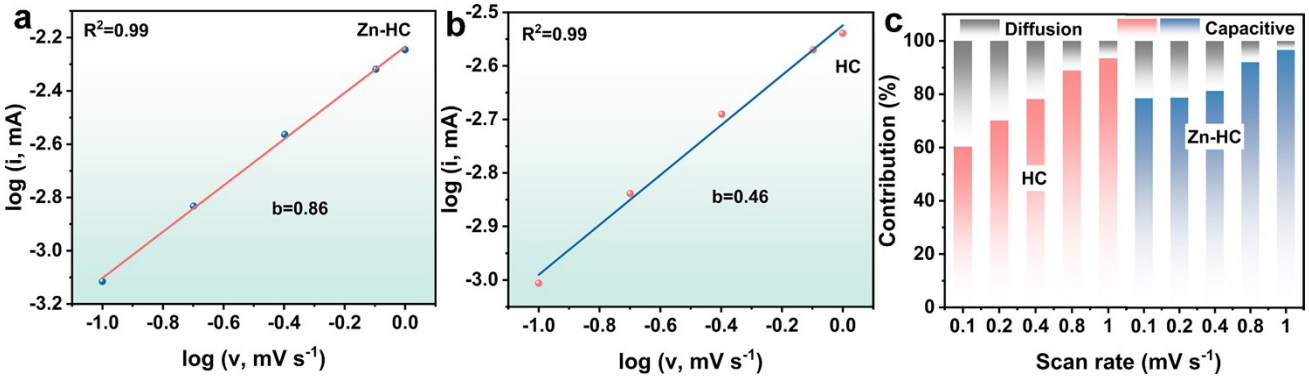

Fig. S13 *b* value of peak current (a) Zn-HC and (b) HC, (c) The contribution ratios of capacitance and diffusion control of HC and Zn-HC at 0.1–1 mV s^{-1}.

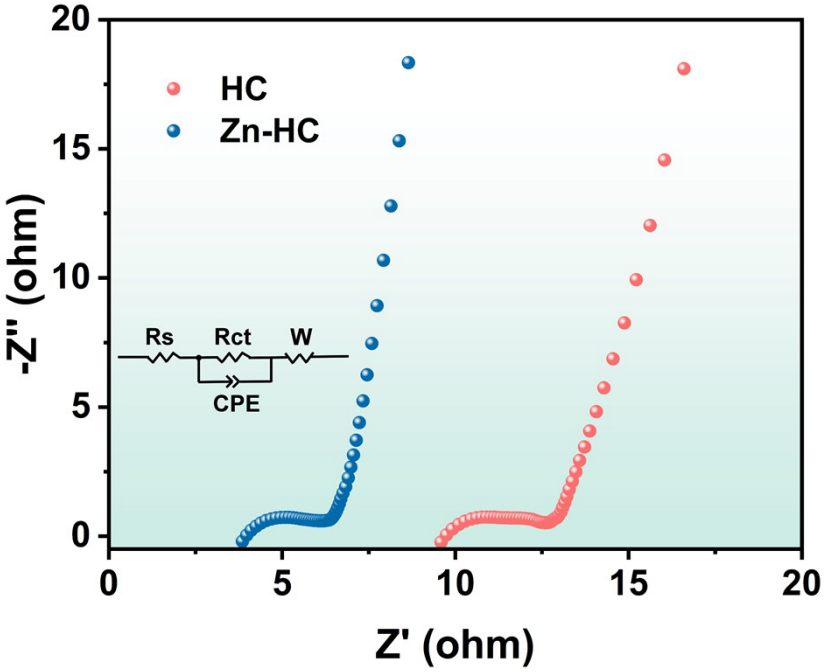

Fig. S14. EIS spectra of Zn-HC and HC.

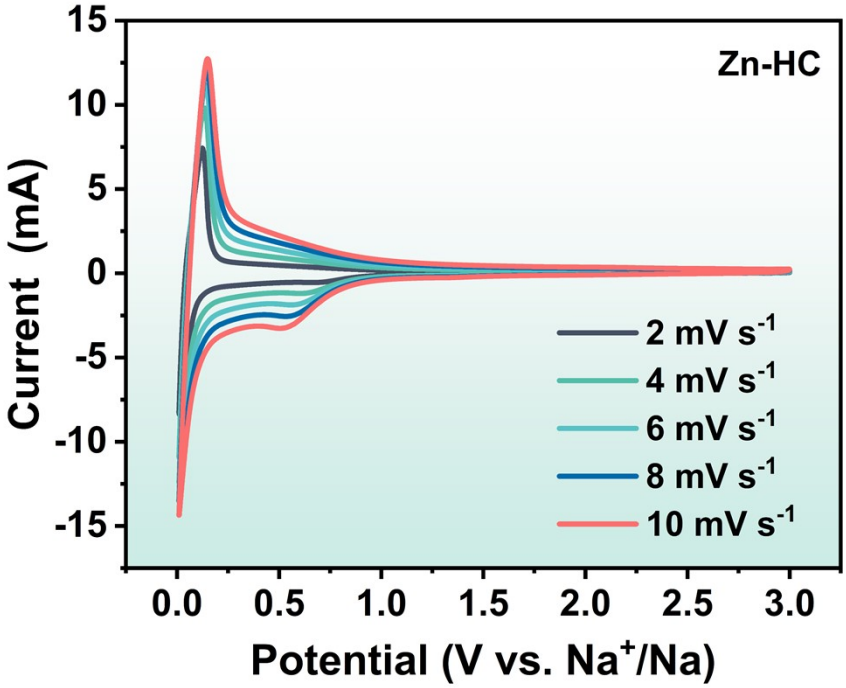

Fig. S15. CV curves of Zn-HC at different scan rates.

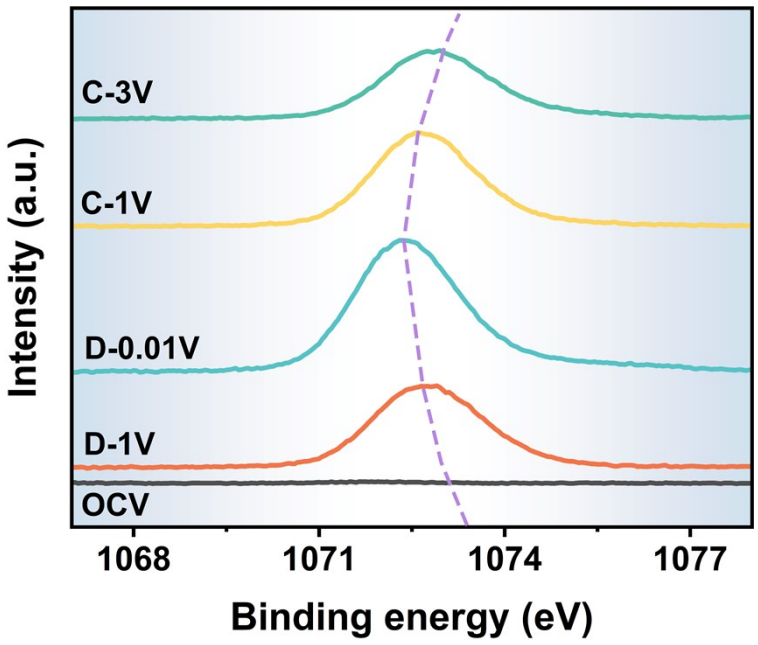

Fig. S16. Ex-situ high-resolution Na 1s spectrum.

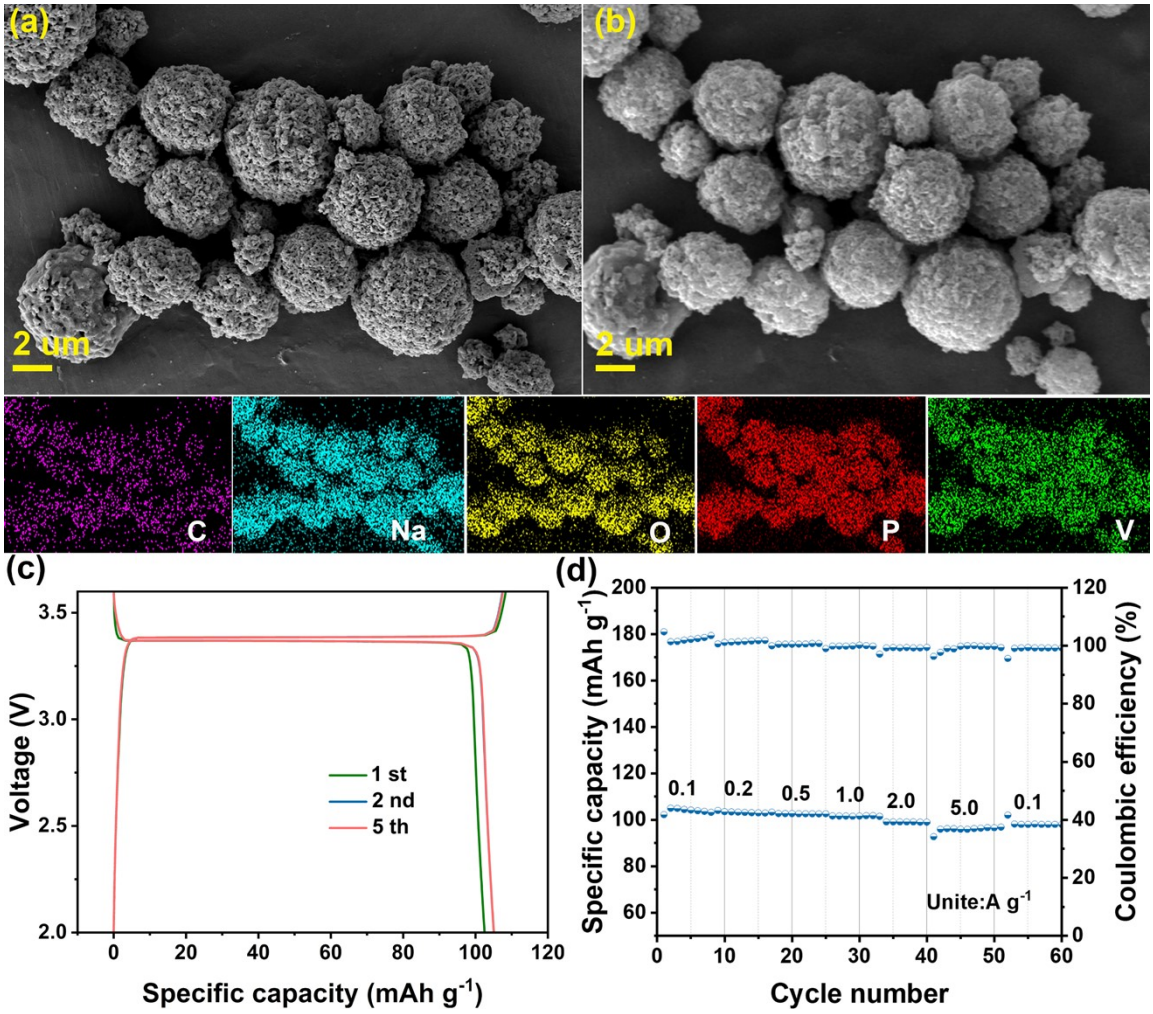

Fig. S17. (a) SEM image, (b) EDS images, (c) GCD curves, and (d) rate performance of NVP@C.

References

[1] Q. He, H. Chen, X. Chen, J. Zheng, L. Que, F. Yu, J. Zhao, Y. Xie, M. Huang, C. Lu, J. Meng and X. Zhang, *Adv. Funct. Mater.*, 2024, **34**, 2310226.

[2] Y. Liu, Y. Wan, J. Zhang, X. Zhang, C. Hung, Z. Lv, W. Hua, Y. Wang, D. Chao and W. Li, *Small*, 2023, **19**, 2301203.

[3] J. Yang, X. Wang, W. Dai, X. Lian, X. Cui, W. Zhang, K. Zhang, M. Lin, R. Zou, K. Loh, Q. Yang and W. Chen, *Nano Micro Lett.*, 2021, **13**, 98.

[4] C. Cai, Y. Chen, P. Hu, T. Zhu, X. Li, Q. Yu, L. Zhou, X. Yang and L. Mai, *Small*, 2022, **18**, e2105303.

[5] Y. Huang, X. Zhong, X. Hu, Y. Li, K. Wang, H. Tu, W. Deng, G. Zou, H. Hou and X. Ji, *Adv. Funct. Mater.*, 2023, **34**, 2308392.

[6] Q. Hu, L. Xu, G. Liu, J. Hu, X. Ji and Y. Wu, *ACS Nano*, 2024, **18**, 21491-21503.

[7] M. Su, K. Zhang, E. Ang, X. Zhang, Y. Liu, J. Yang, Z. Gu, F. Butt and X. Wu, *Rare Metals*, 2024, **43**, 2585-2596.